ARTICLE

Time-dependent Wave Packet Quantum Scattering Study of Reaction $S(^3P)+H_2 \rightarrow HS+H$ on a New *ab initio* Potential Energy Surface $^3A'$

Shuang-jiang Lv, Pei-yu Zhang*, Guo-zhong He

State Key Laboratory of Molecular Reaction Dynamics, Dalian Institute of Chemical Physics, Chinese Academy of Sciences, Dalian 116023, China

(Dated: Received on May 4, 2012; Accepted on May 9, 2012)

A new potential energy surface is presented for the triplet state $^3A'$ of the chemical reaction $S(^3P)+H_2$ from a set of accurate *ab initio* data. The single point energies are computed using highly correlated complete active space self-consistent-field and multi-reference configuration interaction wave functions with a basis set of aug-cc-pV5Z. We have fitted the full set of energy values using many-body expansion method with an Aguado-Paniagua function. Based on the new potential energy surface, we carry out the time-dependent wave packet scattering calculations over the collision energy range of 0.8−2.2 eV. Both the centrifugal-sudden approximation and Coriolis Coupling cross sections are obtained. In addition, the total reaction probabilities are calculated for the reactant H_2 initially in the vibrational states v=0−3 (j=0). It is found that initial vibrational excitation enhances the title reaction.

Key words: Potential energy surface, Quantum-scattering, Time-dependent wave packet

I. INTRODUCTION

The potential energy surface (PES) and quantum scattering dynamics studies of chemical reactions play a very important role in the interpretation of the reaction mechanism. The $S(^3P)+H_2$ reaction, one of the simplest hydrogen abstraction reaction, is of considerable interest in combustion and atmospheric chemistry. In previous work, we have constructed the PES for the ground triplet state $^3A''$ of SH_2 [1], which features an activation barrier on the reaction path. Based on it, we performed exact quantum scattering calculations for the reactions H+HS [1], which shows a direct dynamics mechanism. However, the electronic state $^3A'$ has been less extensively investigated. In fact, the study of the reaction $S(^3P)+H_2$ on electronic state $^3A'$ is important because it is a simple reaction involving sulfur atoms and it is a prototype for hydrogen-atom abstraction reaction studies. In this work, we constructed the accurate PES for studying the dynamics of the reaction $S(^3P)+H_2 \rightarrow HS+H$ on the electronic state $^3A'$.

The full physical system of the reaction $S(^3P)+H_2$ correlates to three triplet electronic states, which are of $1^3A''$, $2^3A''$, and $^3A'$ symmetry for bent SHH geometries. Recently, work on the reaction $S(^3P)+H_2$ has been paid to the singlet-triplet crossing effects [2−6]. PESs currently available for the $^3A'$ electronic state of the title system have been shown as follows. Maiti *et al.* constructed the $^3A'$ PES to study the importance of intersystem crossing in the $S(^1D, ^3P)+H_2 \rightarrow HS+H$ reaction [5]. In the interaction areas of the $^3A'$ state, the 3D-spline interpolation method was used to construct the PES based on the QCISD(T)-level *ab initio* points and the asymptotic areas were constructed by an LEPS function. The globally smooth PES was switched from the spline-fitted *ab initio* points in the interaction region to the LEPS function near the asymptotes by the switching function. Later, Klos *et al.* obtained the analytical PES for $^3A'$ state based on internally contracted multireference configuration interaction with single and double excitation level including the Davidson's correction with the aug-cc-pVQZ basis set [7]. In this work, we present the results of new *ab initio* calculations of the $^3A'$ PES, which are carried out using multi-reference configuration interaction (MRCI) method and a large basis set. About 8×10^3 *ab initio* points are generated over a range of values of the Jacobi coordinates of the H+HS and S+H_2 systems. The resulting energies are fitted to a many-body expansion.

In this work, we study straightforward and standard computations of the PES for the title reaction, followed by detailed full-dimensional quantum-wave-packet dynamical calculation of the reaction dynamics. We have taken the Coriolis Coupling (CC) effect [8, 9] into account and presented the comparison between the centrifugal-sudden (CS) approximation and CC calculations. Then the vibrational effects for the reactant H_2 are investigated in detail. The present CC calculations and vibrational effects will provide further physical insights into the reaction mechanism.

*Author to whom correspondence should be addressed. E-mail: pyzhang@dicp.ac.cn

II. PES

A. *Ab initio* electronic calculations

The new three-dimension adiabatic PES $^3A'$ has been evaluated using accurate multi-reference configuration interaction (MRCI) method [10−12]. First, we performed the highly correlated complete active space self-consistent-field (CASSCF) calculations [13, 14], and then recovered the dynamics correlation energy by the MRCI method. A large basis set, the aug-cc-pV5Z of Dunning [15] was employed in all calculations. We used eight-electrons-in-ten-orbitals both in the CASSCF and MRCI calculations. The remaining orbital was kept doubly occupied. In the CASSCF and MRCI calculations, equal weights were assigned to each of the four states ($^1A'$, $^1A''$, $^3A'$, and $^3A''$) in the state-averaging calculations. In addition, the multi-reference Davidson correction (+Q) [16] was included to compensate for the effect of the higher-order correlation. All *ab initio* calculations have been performed with the MOLPRO package of *ab initio* programs [17].

The final choice of energies and geometries for the PES is very important in order to enable a proper description of the dynamics of the reaction. In order to include the regions of the surface corresponding to reactants, products, intermediate complexes and all asymptotic regions, the grids were generated in Jacobi coordinates over the S-H_2 product region and H-HS reactant region [1]. The reactant region is defined by 0.7 $a_0 \le R_{H_2} \le 20$ a_0, $0 \le R_{S-H_2} \le 20.0$ a_0, and $0.0° \le \theta \le 90°$. For the H-HS product region, a grid defined by 1.6 $a_0 \le R_{SH} \le 8.0$ a_0, $0 \le R_{H-SH} \le 20.0$ a_0 and $0.0° \le \theta \le 180°$ was chosen. In the procedure of generating the fits to the *ab initio* points, we took about 6.6×10^3 *ab initio* energies below 3.8 eV relative to the energy of the S−H−H dissociation limit.

B. Analytical representation of the PES

For the global analytical surface of the title system, we use the many-body expansion in the Aguado-Paniagua function form [18],

$$\begin{aligned} V_{ABC}(R_{AB}, R_{AC}, R_{BC}) = {} & V_A^{(1)} + V_B^{(1)} + V_C^{(1)} + \\ & V_{AB}^{(2)}(R_{AB}) + V_{AC}^{(2)}(R_{AC}) + \\ & V_{BC}^{(2)}(R_{BC}) + \\ & V_{ABC}^{(3)}(R_{AB}, R_{AC}, R_{BC}) \end{aligned} \quad (1)$$

where R represents the pairwise interatomic distance between the three atoms, and $V^{(1)}$, $V^{(2)}$, and $V^{(3)}$ are the one-, two-, and three-body potentials, respectively. The one-body term ($V_A^{(1)}$, $V_B^{(1)}$, and $V_C^{(1)}$) is a constant that is assigned to the value of the separated atom and taken to be zero. The two-body term is written as follows:

$$V_{AB}^{(2)} = c_0 \frac{\exp(-\alpha_{AB} R_{AB})}{R_{AB}} + \sum_{i=1}^{L} c_i \rho_{AB}^i \quad (2)$$

$$\rho_{AB} = R_{AB} \exp(-\beta_{AB} R_{AB}) \quad (3)$$

R_{AB} (R_{AC}) and R_{BC} correspond to the bond lengths of the diatomic systems involved. Here α and β are the exponential parameters and (c_0, ..., c_i) are the linear parameters. The two-body term is fitted first and the optimized parameters are then used for the three-body potential. The three-body term is

$$V_{ABC}^{(3)}(R_{AB}, R_{AC}, R_{BC}) = \sum_{ijk}^{M} d_{ijk} \rho_{AB}^i \rho_{AC}^j \rho_{BC}^k \quad (4)$$

where the indices i, j, and k vary from zero to a maximum value such that $i+j+k \le M$ and $i+j+k \ne i \ne j \ne k$. As there are two identical atoms in the present case (B=C), only two nonlinear parameters need to be determined. The Levenberg-Marquardt technique was used for the nonlinear optimization. For M=12, there are 227 linear parameters to be determined.

C. Characteristics of the analytical potential energy surface

Using the procedure described by Aguado *et al.* [20], we constructed a highly accurate PES. For the two-body terms, 170 points were used to determine the parameters in Eq.(2). The root-mean-square (rms) error was 0.029 kJ/mol for the reagent channel and 0.013 kJ/mol for the product channel.

As for the three-body term, the rms error was 2.47 kJ/mol for the $^3A'$ surface and the maximum energy deviation was 19.06 kJ/mol. Four views of the $^3A'$ surface of different approach of S(^{3}P) to H_2 in internal coordinates are presented in Fig.1. In each view, θ_{S-H-H} is frozen at the specified value, which corresponds to 180°, 120°, 90°, and 60°, respectively. It can be seen that the Aguado-Paniagua function form yields a smooth, well-behaved potential surface for this system. A further check on the smoothness of the surface is provided by the time-dependent wave packet (TDWP) scattering calculations. The first-order derivate of the PES with respective to three bond lengths is also available. It will be interesting in future to carry out the quasi-classical calculations to check the smooth of the PES. It is clear that the minimum energy path occurs at the collinear approach of S(^{3}P) to H_2. The height of barrier increases quickly and the location of barrier shifts from products to reactants when the S−H−H bond angles are decreased from 180° to 60°. The transition state is found to be linear with R_{HH}=2.34 a_0 and R_{HS}=2.67 a_0. The barrier height is 101.57 kJ/mol with respect to the reactant S(^{3}P)+H_2 asymptote, which is 4.18 kJ/mol lower than that of PES in Ref.[5].

DOI:10.1088/1674-0068/25/03/291-296

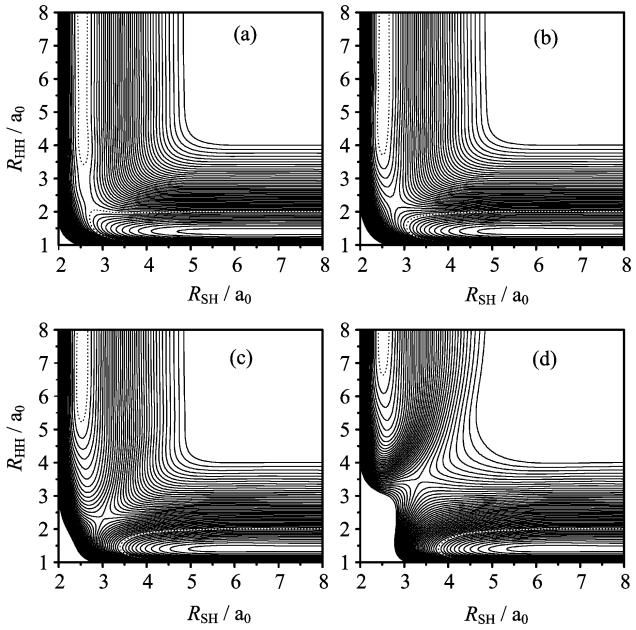

FIG. 1 Contour plots of the potential energy surface for the different S−H−H angles in internal coordinates, (a) 180°, (b) 120°, (c) 90°, (d) 60°. The spacing between the contour lines is 8.36 kJ/mol. The dotted line is 98.14 kJ/mol relative to the energy of the reactant S(^{3}P)+H_2.

III. REACTION DYNAMICS

A. Theoretical method

The TDWP method [21−24] has been widely used in dynamical studies for elucidation of the mechanism of reactive systems, which is the use of the split-operator propagation scheme [25, 26] to numerically solve the time-dependent nuclear Schrödinger equation. For the title reaction, the Hamiltonian expressed in terms of the reactant Jacobi coordinates can be written as

$$H = -\frac{\hbar^2}{2\mu_R}\frac{\partial^2}{\partial R^2} + \frac{(\hat{J}-\hat{j})^2}{2\mu_R R^2} + \frac{\hat{j}^2}{2\mu_r r^2} + V(R,r) + h(r) \quad (5)$$

where R and r have their usual definitions in Jacobi coordinates [21], μ_R and μ_r are the reduced mass of S with respect to H_2 and the reduced mass of H_2, respectively. J and j are the total angular momentum and the rotational angular momentum of H_2, respectively, $V(R,r)$ is the potential energy of the title system excluding the diatomic potential of H_2 and $h(r)$ is the diatomic reference Hamiltonian defined by

$$h(r) = -\frac{\hbar^2}{2\mu_r}\frac{\partial^2}{\partial r^2} + V(r) \quad (6)$$

where $V(r)$ is the diatomic potential function for H_2.

The time-dependent wave function is expanded in terms of the body-fixed (BF) translational-vibrational-rotational basis $u_n^v(R)\varphi_v(r)Y_{jK}^{JM\varepsilon}(\hat{R},\hat{r})$, where n and v are indices labeling the translational and vibrational eigenfunctions, M and K are the projection quantum numbers of the total angular momentum J on the space-fixed z-axis and BF z-axis, respectively. ε is the parity of the system.

In the CS approximation calculation, the matrix obtained by applying the centrifugal potential operator $(\hat{J}-\hat{j})^2/2\mu_R R^2$ on the rotational basis functions $Y_{jK}^{JM\varepsilon}(\hat{R},\hat{r})$ is diagonal, while in the CC calculation different K states coupled with each other and constitute the off-diagonal elements of the matrix. To get the converged results, we used 300 translational basis function for the R coordinate in a range of 0.1−16 a_0, 210 vibrational basis functions for the r coordinate of 0.5−15.0 a_0, and j_{max}=100 for rotational basis functions, as well as a propagation time of 8×10^3 a.u. for the wave packet initially on the $^3A'$ state. Here we take the CC effect into account. The number of K used in the CC calculations is up to 2 to provide the fully converged results, where K is the projection of J on the body-fixed z-axis. The reaction cross sections were calculated using all J values in the range $0\leq J\leq J_{max}$, where J_{max}=75 is sufficient to converge the cross sections in the investigated energy range.

The total reaction probability can be extracted by calculating the flux at a fixed surface of the corresponding time-dependent part of the wave function after propagation for a sufficient length of time [21],

$$P_{v_0j_0k_0}^J(E) = \frac{\hbar}{\mu_r}\mathrm{Im}[\langle\psi(E)\rangle|\delta(r-r_0)|\langle\psi(E)\rangle] \quad (7)$$

where v_0, j_0, and k_0 (the projection quantum number of j_0) are the initial quantum numbers to denote the initial rovibrational state. The individual and total reaction cross section can be calculated by

$$\sigma_{v_0j_0k_0}(E) = \frac{\pi}{k^2}\sum_J (2J+1)P_{v_0j_0k_0}^J(E) \quad (8)$$

$$\sigma_{v_0j_0}(E) = \frac{1}{2j_0+1}\sum_{k_0}\sigma_{v_0j_0k_0}(E) \quad (9)$$

where k is the wavenumber corresponding to the initial state at a fixed collision energy E and the summations in Eqs. (8) and (9) extend to all possible values of J and k_0, respectively.

B. Results and discussion

We have previously employed the TDWP method to investigate some other reactions, such as Ne+H_2^+ [19] and H+HS [1], on the corresponding adiabatic PES. It should be mentioned that due to spin-orbit coupling in the S atom, the S(^{3}P)+H_2 reaction as well as O(^{3}P)+H_2

DOI:10.1088/1674-0068/25/03/291-296

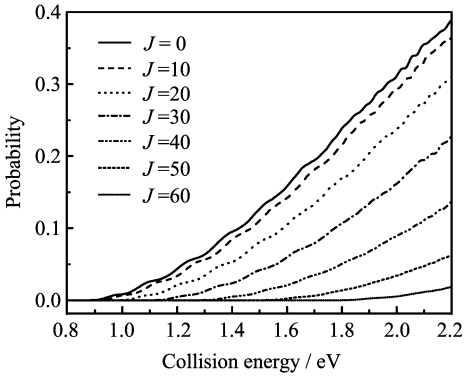

FIG. 2 The centrifugal-sudden calculated reaction probabilities as a function of collision energy for the reactant H_2 initially in the ground rovibrational state for total angular momentum J.

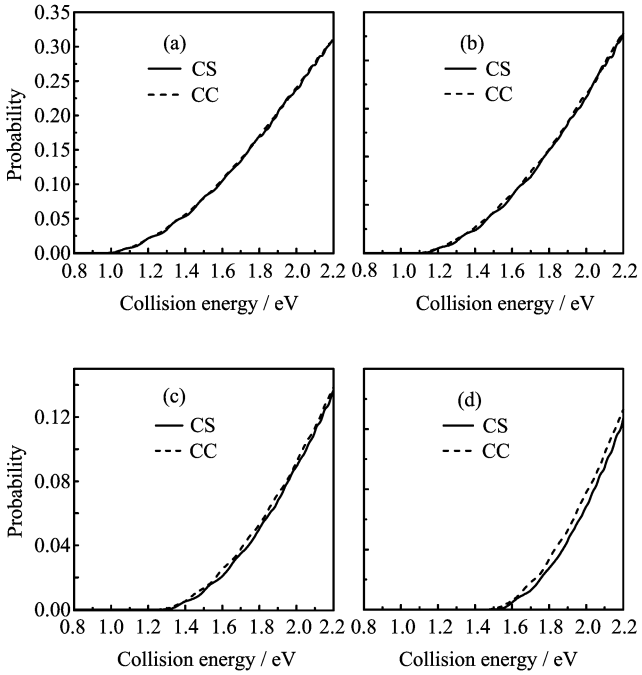

FIG. 3 Comparison between the CC and CS probabilities in the collision energy for initial quantum numbers j=0, v=0, and for total angular momenta. (a) J=20, (b) J=30, (c) J=40, (d) J=50,

reaction [27−29] involves several electronic states. Recent trajectory surface-hopping [5] and TDWP studies [8] that include spin-orbit-induced intersystem crossing effects have been investigated, which shows that the nonadiabatic effects play an important role in the S(^{1}D, ^{3}P)+H_2/HD reactions. However, the branching ratio $\sigma_{SH+D}/\sigma_{SD+H}$ [8] is larger than the experimental results of Liu and co-workers [30], which may be attributed to the PESs ^{3}A″ or ^{3}A′ in the nonadiabatic calculations [8]. Here we carry out the dynamics calculations on the adiabatic ^{3}A′ state to check the quality of our new PES. In future the nonadiabatic dynamics calculations can be perform based on the present ^{3}A′ PES and recent ^{3}A″ PES in Ref.[1].

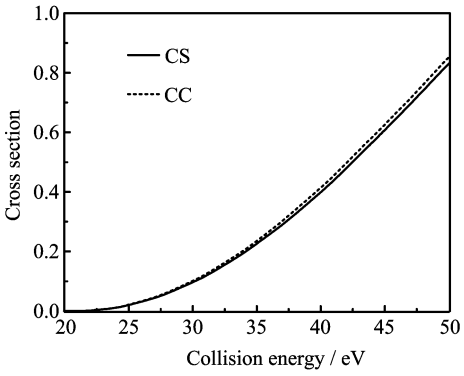

FIG. 4 Calculated CS and CC total reactive cross sections as a function of collision energy for reactant H_2 in its ground rovibrational state.

In Fig.2, we present the CS calculated reaction probabilities in the collision energy E_{col} range of 0.8−2.2 eV, and the reactant H_2 set initially in its ground rovibrational state for the total angular momentum J=0, 10, 20, *etc.* All reaction probabilities are relatively smooth and tend to increase monotonically with increasing collision energy because the PES is quite simple, showing a straight uphill and downhill in the route to produce the HS molecule, a feature suggesting that a direct dynamics should take place in this electronic state. It is noted that the threshold energy for J=0 is about 0.92 eV, which is smaller than the barrier of the PES. This fact is attributed to the zero point energies at the reactant and saddle point. Moreover, the reaction threshold progressively shifts toward the higher collision energy with increasing J because the centrifugal barrier also increases with J.

Extensive convergence tests have been performed with respect to the K blocks (the computational parameters) before quantum scattering calculations with Coriolis couplings are carried out. The number of K used in the CC calculations is up to 2 to provide the fully converged results.

Figure 3 shows the CC and CS probabilities for initial quantum numbers v=0, j=0, and total angular momentum J=20, 30, 40, and 50, respectively, for the collision energy range 0.8−2.2 eV. It can be seen that the differences between the CC and CS probabilities are rather small for low J values, such as J=20, 30, and 40; but as J becomes larger, for example, J=50, more differences are observed. Note that the CC values are a bit larger than the CS values within the whole energy range. However, the differences are rather small for most of J values although remarkable differences (about 10%) are observed for J=50.

Figure 4 shows the calculated CS and CC total reactive cross sections as a function of collision energy for reactant H_2 in its ground rovibratinal state. Values of

DOI:10.1088/1674-0068/25/03/291-296

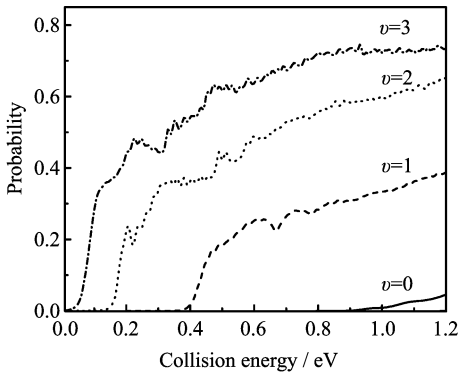

FIG. 5 The total reaction probabilities for the S(^{3}P)+H_2 (v=0−3, j=0) as a function of collision energy for total angular momentum J=0.

J from 0 to 75 are included in Eq.(9) in evaluating the cross sections. In the low-energy region below ∼1.2 eV, there is a good agreement between the CS and CC results while the CC cross section is always slightly larger (about 0−8%) than the CS one in the high-energy region. Indeed, despite some quantitative differences concerning the apparent tendency of the CC curve to lie on the above the CS one, there is generally good qualitative agreement. It seems then safe to conclude that the cheaper CS approximation performs well for the title reaction.

Figure 5 shows the CS reaction probabilities for initial vibrational states v=0−3 (j=0) for the total angular momentum J=0. The reaction threshold progressively shifts toward the lower collision energy with increasing v and no threshold energy is found at v=3. The probability for v=0−3 (j=0) is 0.044, 0.388, 0.650, and 0.736, respectively, at $E_{\rm col}$=1.2 eV. So it can be concluded that the vibrational excitation has appreciable effect on the reaction threshold and causes an increase of the probabilities. The properties of the saddle point for the collinear configuration indicate that the title system presents a late barrier ($R_{\rm SH}-R_{\rm e,SH}$=0.13 Bohr, $R_{\rm HH}-R_{\rm e,HH}$=0.94 Bohr). The vibrational excitation of reactants is favored because of the late barrier character.

IV. CONCLUSION

A new potential energy surface for the state ^{3}A′ of the title reaction has been constructed from high-quality *ab initio* data, which were calculated using the high-level multireference (MRCI+Q) method for the augmented correlation consistent quintuple zeta basis set of Dunning. We have performed a three-dimensional TDWP scattering calculation on the new potential energy surface. The comparison between the CS and CC cross sections for initial quantum numbers v=0 and j=0 suggests that the cheaper CS approximation may perform well for the title system. The total reaction probabilities are calculated for initial state v=0, 1, 2, and 3 as a function of collision energy. It predicts a very important enhancement of reactivity with reagent vibrational excitation, with agreement late barrier character.

The ^{3}A′ PES reported here is based on high-quality *ab initio* calculations, which will serve as a benchmark for multiple-surface calculations in future. The computer code of the new PES can be made available upon request to the authors.

V. ACKNOWLEDGMENTS

This work was supported by the National Key Basic Research Special Foundation of China (No.2007CB815202) and the National Natural Science Foundation of China (No.21021004 and No.20833008).

[1] S. J. Lv, P. Y. Zhang, K. L. Han, and G. Z. He, J. Chem. Phys. **136**, 094308 (2012).
[2] D. Woiki and P. Roth, J. Phys. Chem. **98**, 12958 (1994).
[3] H. Shiina, M. Oya, K. Yamashita, A. Miyoshi, and H. Matsui, J. Phys. Chem. **100**, 2136 (1996).
[4] H. Shiina, A. Miyoshi, and H. Matsui, J. Phys. Chem. A **102**, 3556 (1998).
[5] B. Maiti, G. C. Schatz, and G. Lendvay, J. Phys. Chem. A **108**, 8772 (2004).
[6] T. S. Chu, K. L. Han, and G. C. Schatz, J. Phys. Chem. A. **111**, 8286 (2007).
[7] J. A. Kłos, P. J. Dagdigian, and M. H. Alexander, J. Chem. Phys. **127**, 154321 (2007).
[8] T. S. Chu and K. L. Han, Phys. Chem. Chem. Phys. **10**, 2431 (2008).
[9] E. L. Wu, J. Comput. Chem. **31**, 2827 (2010).
[10] P. J. Knowles and H. J. Werner, Chem. Phys. Lett. **145**, 514 (1988).
[11] H. J. Werner and P. J. Knowles, J. Chem. Phys. **89**, 5803 (1988).
[12] P. J. Knowles and H. J. Werner, Theor. Chim. Acta **84**, 95 (1992).
[13] P. J. Knowles and H. J. Werner, Chem. Phys. Lett. **115**, 259 (1985).
[14] H. J. Werner and P. J. Knowles, J. Chem. Phys. **82**, 5053 (1985).
[15] R. A. Kendall, T. H. Dunning, and R. J. Harrison, J. Chem. Phys. **96**, 6796 (1992).
[16] E. R. Davidson and D. W. Silver, Chem. Phys. Lett. **52**, 403 (1977).
[17] H. J. Werner, A. Berning, D. L. Cooper, M. J. O. Deegan, A. J. Dobbyn, F. Eckert, C. Hampel, T. Leininger, R.Lindh, A. W. Lloyd, W. Meyer, M. E. Mura, A. Nickla, P. Palmieri, K.Peterson, R. Pitzer, P. Pulay, G. Rauhut, M. Schfltz, H. Stoll, A. J. Stone, and T. Thorsteinsson, *MOLPRO Version 2006.1, a Package of ab initio Programs*, (2006), http://www.molpro.net/.

DOI:10.1088/1674-0068/25/03/291-296

[18] A. Aguado and M. Paniagua, J. Chem. Phys. **96**, 1265 (1992).
[19] S. J. Lv, P. Y. Zhang, K. L. Han, and G. Z. He, J. Chem. Phys. **132**, 014303 (2010).
[20] A. Aguado, C. Tablero, and M. Paniagua, Comput. Phys. Commun. **108**, 259 (1998).
[21] J. Z. H. Zhang, *Theory and Application of Quantum Molecular Dynamics*, Singapore: World Scientific, (1999).
[22] D. H. Zhang and J. Z. H. Zhang, J. Chem. Phys. **101**, 3671 (1994).
[23] T. S. Chu, Y. Zhang, and K. L. Han, Int. Rev. Phys. Chem. **25**, 201 (2006).
[24] R. F. Lu, P. Y. Zhang, T. S. Chu, T. X. Xie, and K. L. Han, J. Chem. Phys. **126**, 124304 (2007).
[25] J. A. Fleck, J. R. Morris, and M. D. Feit, Appl. Phys. **10**, 129 (1976).
[26] R. F. Lu, T. S. Chu, and K. L. Han, J. Phys. Chem. A **109**, 6683 (2005).
[27] T. S. Chu and K. L. Han, J. Phys. Chem. A **109**, 2050 (2005).
[28] B. R. Han and Y. J. Zheng, J. Comput. Chem. **32**, 3520 (2011).
[29] B. Maiti and G. C. Schatz, J. Chem. Phys. **119**, 12360 (2003).
[30] S. H. Lee and K. P. Liu, Chem. Phys. Lett. **290**, 323 (1998).

DOI:10.1088/1674-0068/25/03/291-296